Rutherford scattering and heavy-ion reaction study

Anushree Ghosh, Nitali Dash, Sudeshna DasGupta, Sumanta Pal & Vivek Singh

INO GRADUATE SCHOOL

1 Introduction:

To probe the properties of the nuclei and predict their behavior scattering of nuclei at different energies is done. Study of nucleon-nucleon scattering above E >E_c opens the channel of nuclear reactions and inelastic scattering which provides an insight in the nuclear structure. In this project, a study of Rutherford scattering and angular distribution for ^{12}C+^{209}Bi below and above E_c (at lab energies of 48MeV and 66MeV respectively) was carried out. While the first conformed to the ideal Rutherford scattering, the later was analyzed in the framework of the optical model. The Wood-Saxon potential volume parameters were extracted for the same. At E >E_c apart from the usual elastic scattering, direct reactions and compound nuclear reactions also take place. This is illustrated here using ^{12}C+^{27}Al scattering, at 66MeV, where the light particles produced in the reaction were identified. The quantum effect of identical particle scattering, which has no classical analogy, was also studied. The difference between the identical and distinguishable particle scattering was illustrated by comparing the ^{12}C+^{12}C with ^{13}C+^{12}C scattering at projectile energy of 20MeV.

2 Experimental Setup

The beam was taken from 14MV TIFR-BARC Pelletron accelerator facility at TIFR, Mumbai. The targets used were in the form of self supporting foils. The target and the detector were mounted inside the scattering chamber of 1m diameter for measuring the projectile particles under high vacuum of $\sim 10^{-5}$mbar. A schematic diagram of experimental set up is shown in Figure 1. The incident beam was collimated with a 5mm diameter aperture. The detector was mounted on a movable arm inside scattering chamber and the targets were mounted on an adjustable ladder. A $\triangle$E-E telescope detector was used for energy measurement and particle identification. A Silicon surface barrier detector of thickness 30μm (transmission mount) was used as a $\triangle$E detector while the E detector had a thickness of 300μm (back mount). The detector system was collimated with a 5mm diameter aperture for particle acceptance and was mounted at 21cm distance from the target ladder subtending a solid angle of 0.49 mrad at the target.

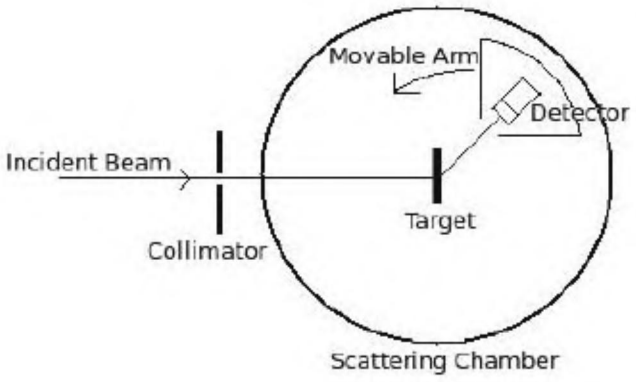

Figure 1: Schematic of experimental setup.

The angle off set was corrected by scanning the angles with a step size of $\frac{1}{2}^0$ at the forward angle of 20^0 on either side of the beam. By comparing the yield value on both sides angle offset was found out to be 1.6^0. Fast coincidence between $\triangle$E and E was used to generate an event trigger and energies of both the detectors were recorded using a CAMAC based acquisition system (LAMPS). The gain and shaping time of amplifiers were adjusted to get the best signal to noise ratio. The CFD threshold were set just above the noise level. A schematic diagram of the electronics setup is shown in Figure 2. Typical counting time of 15-90 minutes were used to get reasonable statistics. Beam current was measured using a Faraday Cup. Typical beam current of 20-65 nA was used. The beam energy was set by the analyser magnet. Magnetic field was calculated without considering relativistic correction.

$$B = k\frac{\sqrt{EA}}{q} \tag{1}$$

where k=720.44$\pm$0.01, a system constant for the magnet used, E is the incident beam energy, "A" is the mass number of the projectile particle and "q" is the charge state.

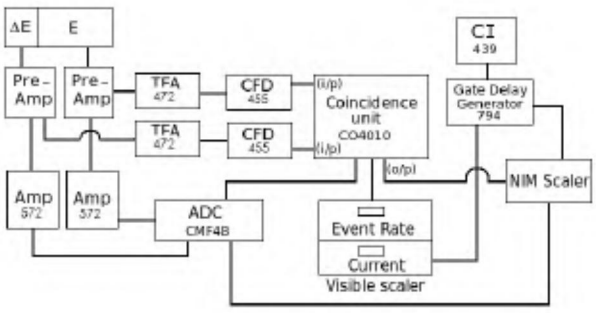

Figure 2: Schematic of electronics setup.

The typical accelerator parameters for a beam are listed in Table 1.

Incident Particle	Charge State	Voltage (MV)	Magnetic Field of Analyzing Magnet (Gauss)	Beam Energy (MeV)
^{12}C	5^+	8.0	3458.11	48
^{12}C	5^+	11.0	4054.99	66
^{13}C	4^+	4.0	2904.19	20
^{12}C	4^+	4.0	2790.25	20

Table 1: The typical accelerator beam parameters

3 Rutherford Scattering

The Rutherford scattering on ^{209}Bi target was done with ^{12}C beam at 48MeV (E <E_c) and 66MeV (E >E_c). The targets were prepared using vacuum evaporation technique and the thickness was measured using thickness monitor. The thickness was independently measured by the energy loss method with an ^{241}Am α-source to be 275$\pm$10μg/cm^2. The elastic scattering angular measurement was done in the range of θ_{lab}= 20^o- 150^o with the angular resolution being about 0.5^o. Coincidence between $\triangle E$ and E was set up to identify the charge and mass separated products from 2D spectrum of $\triangle E$ versus $\triangle E + E$. The differential scattering cross section, normalized to the Rutherford scattering, is shown in Figure 3. For forward scattering angle and in angular range below and near the barrier the statistical error on the normalized cross section is about 1% while towards backward angles it is 3%. The values of σ_{el}/σ_R at different scattering angles for E_{lab}= 48MeV shows that below the coulomb barrier the nuclei can only undergo elastic scattering under the influence of nuclear force. On the other hand for E_{lab}= 66MeV, σ_{el}/σ_R shows a sharp but continuous fall near the grazing angle. Strong nuclear forces between the colliding nuclei causes significant distortion in all of the projectile trajectories and they are removed from the elastic channels because of nuclear absorption. The 66MeV data set were fitted within the framework of optical model using FRESCO[1]. In this model, the incident particle in its encounter with the target nucleus, is acted upon by an average potential which is complex. A volume Woods-Saxon potential

$$V_r = U_c(r, r_c) - \{V(r) + iW(r)\} \quad (2)$$

was used for analysis where V(r)=V$_0$f$_0$ and W(r)=W$_0$f$_1$. The strengths of the real and imaginary potential are given by V$_0$, W$_0$ and

$$f_i = \frac{1}{1 + exp(\frac{r - R_i}{a_i})} \quad (3)$$

where i= 0 or 1. The real part of the potential gives the elastic scattering while the imaginary part gives the absorption term of the incident projectile inside the nucleus. R$_i$ gives the measure of the effective nuclear potential width and is defined as distance between the centers of the two colliding nuclei while a$_i$ gives a measure of diffusiveness in the same. The term U$_c(r, r_c)$ is the coulomb potential between the two nuclei.

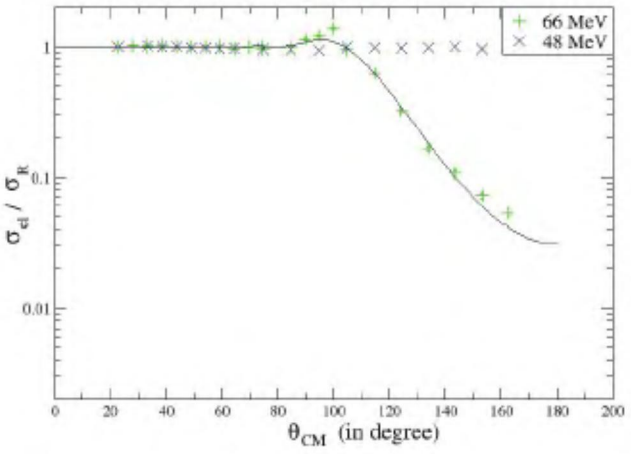

Figure 3: Normalized cross section for ^{12}C+^{209}Bi at 48MeV and 66MeV

The Optical model fit was obtained by minimizing the $\chi^2$for the fit by searching all the parameter space of real and imaginary potential function. The best fit value is shown in Table 2. The broad maxima near the grazing angle is due to the constructive interference between part of the incident particle wave function scattered from the front surface of the nuclear potential well and part scattered from the back. However

the data point near the maxima seems anomalous and needs repeat of the measurement.

V_0(MeV)	R_0(fm)	a_0(fm)	W_0(MeV)	R_1(fm)	a_1(fm)
81.48±0.91	1.255±0.002	0.444±0.001	22.49±2.76	1.294±0.006	0.290±0.012

Table 2: The optical model parameters for Woods Saxon volume Potential for ^{12}C+^{209}Bi at E_{lab}= 66MeV.

4 Nuclear Reaction

^{12}C beam of E_{lab}= 66MeV was bombarded on ^{27}Al target to study heavy ion reaction process. The target thickness was 0.965mg/cm^2. The $\triangle$E -E telescope detector was kept at a lab angle of 30^o with respect to the beam. As before, the 2D spectrum of $\triangle E$ versus $\triangle E + E$ was used to identify the charge and mass separated reaction products. The 2D spectrum is shown in Figure 4. The particle identification was done using the fact that $\triangle E \propto \frac{Z^2}{\beta^2} \sim MZ^2/E_{total}$ where E_{total} is $(\triangle E + E)$. The particles identified were $^{14}N_7$, $^{12}C_6$,$^{11}B_5$, $^{10}B_5$,$^{9}Be_4$,$^{7}Be_4$, $^{7}Li_3$, $^{6}Li_3$,$^{4}He_2$. It therefore, shows that for energies E > $E_{coulomb}$ the incident trajectories which can cross the barrier are trapped in the nuclear potential pocket and fuse with the scatterer to form a single, equilibriated compound nucleus (CN). This nucleus subsequently decays either by evaporation of light particles or emission of intermediate mass fragments.

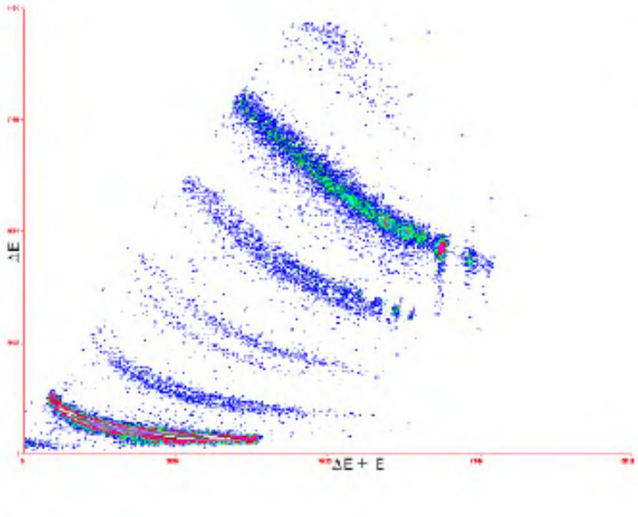

Figure 4: $\triangle E$ vs $(\triangle E + E)$ for particle identification

The first and second excited states of ^{12}C (4.438MeV and 7.654MeV respectively) were identified. The first, second and third excited states of ^{11}B(2.124MeV, 4.444MeV and 5.02MeV respectively) were also observed. The $\triangle E$ detector thickness was also confirmed from the punch back of $^{4}He_2$ spectra which appeared at 28MeV. Stopping range of $^{12}C_6$ beam at energy 28MeV for Al target was estimated using SRIM and it was appeared almost 30μm.

5 Identical Particle Scattering[2]

^{12}C target was bombarded with 20MeV beam of ^{12}C and ^{13}C respectively. The first is the collision of two identical spinless nuclei while the latter is collision between distinguishable particles though the coulomb interaction due to charge Ze remain the same in both the cases. The targets were prepared using vacuum evaporation technique and the thickness was measured using thickness monitor. The thickness was independently measured by the energy loss method with an ^{241}Am α-source to be 67±10μg/cm^2. The scattering angular measurement was done in the range of θ_{lab}≈20^o- 70^o with the angular resolution of about 0.5^o. The cross sections are normalized to the forward scattering angle of θ_{lab}=21.6^o. The comparison between theoretical and experimental plot for normalized cross section for both ^{12}C+^{12}C and ^{12}C+^{13}C is shown in Figure 5 and Figure 6 respectively.

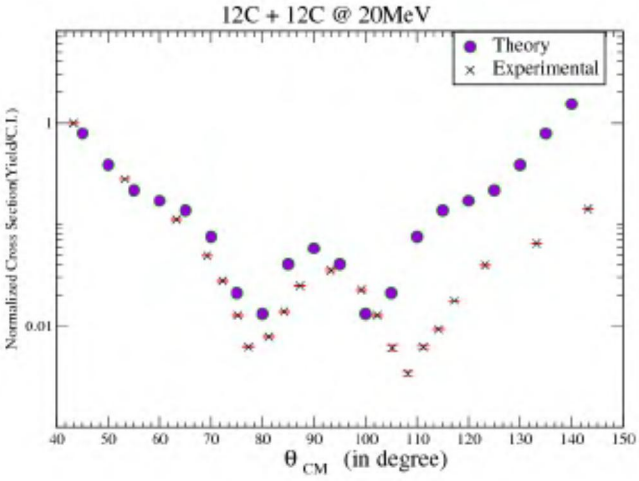

Figure 5: Normalized cross section (theoretical & experimental)for ^{12}C+^{12}C E_{lab}= 20MeV.

For ^{12}C+^{13}C scattering Figure 6 shows the total cross section due to detection of both ^{12}C and^{13}C. Classicaly the differential scattering cross section for distinguishable particle in central interaction potential is defined as

$$\left(\frac{d\sigma}{d\Omega}\right)_{distinct} = |f(\theta)|^2 + |f(\pi - \theta)|^2 \qquad (4)$$

which is the sum total of the differential scattering cross section of both the nuclei. ^{12}C+^{13}C clearly validates this as the cross section first decreases to a minima around θ_{CM}=90^{o}and again increases.

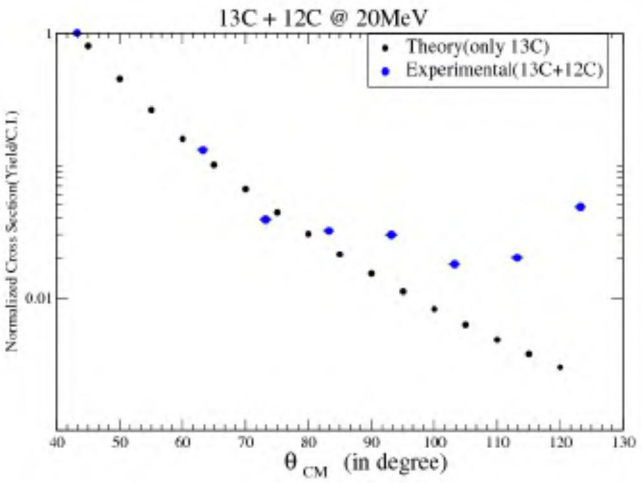

Figure 6: Normalized cross section (theoretical & experimental) for ^{12}C+^{13}C at E_{lab}= 20MeV.

However in case of identical particles scattering^{12}C+^{12}C, due to symmetry under the interchange of spatial co-ordinates of two particles, the differential cross section now contains an interference term, which has no classical analogy, and is given by

$$\left(\frac{d\sigma}{d\Omega}\right)_{identical} = |f(\theta) + f(\pi - \theta)|^2 \qquad (5)$$

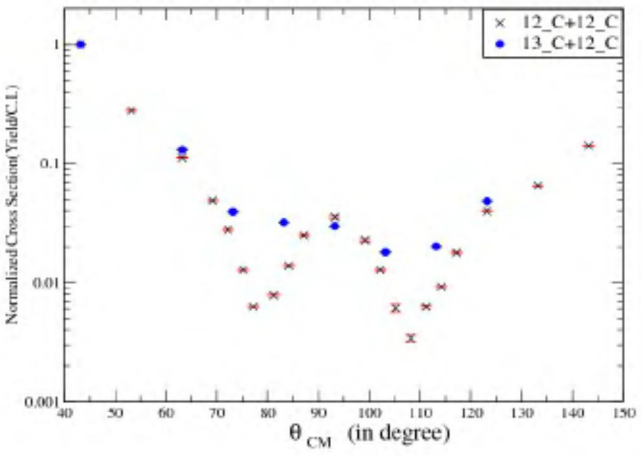

Figure 7: Normalized cross section for ^{12}C+^{12}C and ^{12}C+^{13}C at E_{lab}= 20MeV.

The interference term peaks at θ_{CM}=90^o as can be seen from the ^{12}C+^{12}C cross section data. It should be noted that the beam energy of 20MeV is higher than the coulomb barrier of the respective systems and hence the nuclear forces between the two colliding nuclei cannot be neglected. The reduced elastic cross section above the grazing angle θ_{CM}≈103^o strongly hints at the presence of nuclear couplings.

6 Conclusion

Elastic scattering measurements are reported for the system ^{12}C+^{209}Bi for energy scale of 48MeV and 66MeV. The optical model (phenomenological) analysis was done using FRESCO and the fitted values of optical model are nearly in agreement with Santra et. al[3]. The fact that nuclear reaction channels open up for collision above Coulomb barrier was shown using ^{12}C+^{27}Al. The interference term for identical particle scattering was clearly established and distinguished with the classical scattering of two particles.

7 References

1. FRESCO, I.J.Thompson, Version FRES 2.4, Dec 2007

2. Treatise on Heavy-Ion Science, Vol-3, Chapter-3, Page-231, ^{12}C+^{12}C angular distribution and phase shift analysis of the MIT Group.

3. S. santra, P. singh, S. Kailas, A. Chatterjee, A. Navin, A. Shrivastava, A.M. Samant and K. Mahata, Phys. Rev. C, 60,034611(1999).